ACS APPLIED MATERIALS & INTERFACES

Research Article

www.acsami.org

# Polydopamine As an Efficient and Robust Platform to Functionalize Carbon Fiber for High-Performance Polymer Composites

Shusheng Chen, Yewen Cao, and Jiachun Feng*

State Key Laboratory of Molecular Engineering of Polymers, Department of Macromolecular Science, Fudan University, Shanghai 200433, China

Supporting Information

**ABSTRACT:** Carbon fibers (CFs), which exhibit excellent physical performances and low density, suffer from their low surface activity in some application. Herein, based on dopamine chemistry, we proposed an efficient method to functionalize them: through a simple dip-coating procedure, the CFs were inverted from amphiphobic to hydrophilic with deposition of polydopamine film. Furthermore, using polydopamine as a bridge, the hydrophilic functionalized CFs were transformed to be oleophilic after following octadecylamine grafting. To illustrate applications of this functionalization strategy, we added 15 wt % functionalized CFs into polar epoxy and nonpolar poly(ethylene-co-octene), and as a consequence, their tensile strength respectively increase by 70 and 60%, which show greater reinforcing effect than the unmodified ones (35 and 35%). The results of dynamic mechanical analysis and scanning electron microscope observations indicate that this polydopamine-based functionalization route brought about satisfactory improvements in interfacial adhesion between fillers and matrix. Considering that this simple approach is facile and robust enough to allow further specific functionalization to adjust surface properties, these findings may lead to the development of new efficient strategies for surface functionalization of CFs that are of great interest to the industrial field.

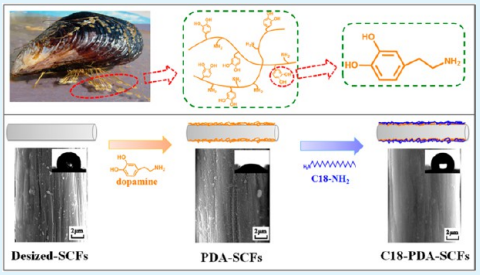


**KEYWORDS:** *carbon fiber, dopamine, interfacial adhesion, polymer-based composites*

## 1. INTRODUCTION

Carbon fibers (CFs) have become one of ideal reinforcements for polymer matrix composites because of their excellent mechanical properties and low weight. As is well-known, effective reinforcement requires good bonding between fibers and matrix, especially in the case of short fibers.[1] However, the surface of an untreated carbon fiber consists of graphitic basal planes and edge sites, with a few small, weakly bound crystallites left over from the graphitization process, which make it suffer from miniature active specific surface area, low surface energy, and surface amphiphobic property. As a result, it is difficult for CFs to be wetted and almost impossible to chemically bond to most polymer matrices, including polar and nonpolar polymers.[2−4] Over the past decades, a great number of scientific works have been done on surface modification of CFs to improve the interfacial interaction between fibers and polymer matrices. These works include surface treatments with various dry and wet oxidation methods,[5,6] electrochemical oxidation,[7,8] plasma treatment,[9,10] and fiber sizing or coating.[11,12] With respect to traditional chemical treatments, such as oxidation methods and plasma treatment, weak outer layers on the fiber are removed and chemical bonding between fibers and matrices is formed by increasing the number of surface active groups.[13] However, these treatments would damage the mechanical properties of fibers to some extent.[14] Compared with chemical treatments, fiber sizing or coating protects fibers from fuzzing and fragmenting during composite processing, preserving or even enhancing their mechanical properties. However, considering the amphiphobic surface of CFs, most sizing agents are not satisfactory in chemical coupling of carbon fiber to the polymer matrices.[13] Therefore, searching for a new strategy for surface functionalization of CFs, which could possess excellent coating and chemical treatment effects, is highly desirable.

Marine mussel adhesive proteins have drawn great interest with their amazing sticking ability. It is believed that 3,4-dihydroxy-L-phenylalanine (L-DOPA) and lysine amino acids (lysine), abundant in the adhesive proteins of mussels, contribute to the adhesive properties of mussels.[15] Recently, Lee at al.[16] found that dopamine, a small-molecule compound, which contains both functionalities of L-DOPA and lysine, can self-polymerize under mild reaction conditions and form polydopamine (PDA) film onto almost all types of inorganic and organic substrates, including "nonsticking surfaces" such as polytetrafluoroethylene. In the past years, a large number of new substrates, such as clay,[17−20] graphene oxide,[21−23] and electrospun nanofibers,[24−26] have been modified using dopamine. Moreover, under oxidizing conditions, the catechols of PDA coating can react with thiols and amines via Michael addition or Schiff base reactions.[27−32] This enables PDA

Received: October 6, 2013
Accepted: November 14, 2013
Published: November 14, 2013

  

**Scheme 1. Schematic Description of Surface Functionalization of Carbon Fibers and Fabrication of Polymer Composites**

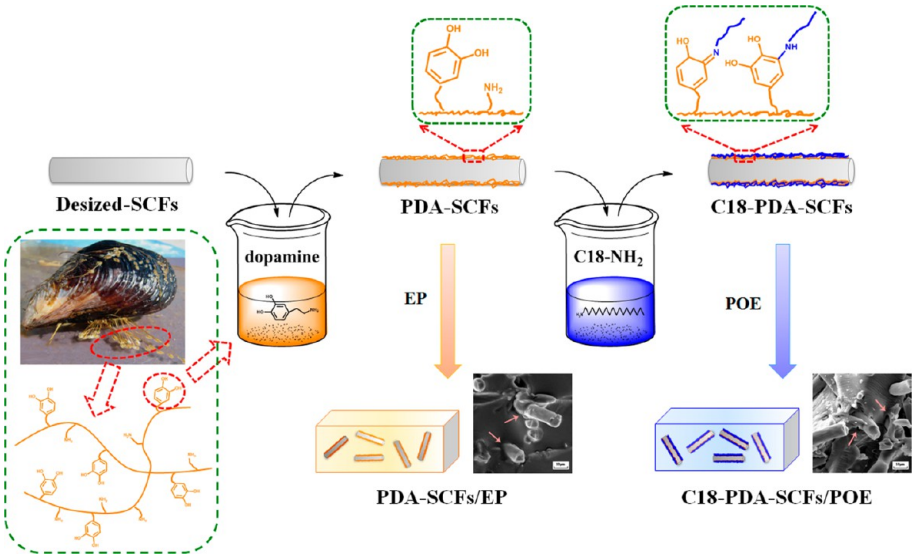


coating to serve as a versatile platform for further specific functionalization, thus opening up the possibility of tailoring the coating for various applications. For instance, Lu et al.[17,18] improved the hydrophilicity of clay by coating it with PDA film. Similarly, a hydrophobic and superoleophilic stainless steel mesh has been prepared by Cao et al.[33] via mussel-inspired chemistry. In our previous work, we successfully controlled the cross-link reaction between PDA-capped graphene oxide and PEI by tuning the pH of the system.[23] Expectedly, on the basis of dopamine chemistry, amphiphobic substrates such as CFs can be facilely transformed to hydrophilic substrates by depositing with PDA film. Further specific functionalization can also be easily achieved dependent on this PDA platform. In particular, this strategy will not cause any damage to the mechanical properties of substrates, which might even be improved during the processing. However, to best of our knowledge, there are few works focusing on the surface functionalization of CFs via dopamine chemistry.

In the present work, we reveal the potential of dopamine to be developed as an effective and robust surface modifier of CFs. The amphiphobic surface of CFs was converted to hydrophilic surface by coating with PDA film. Furthermore, the hydrophilic functionalized CFs became oleophilic after following octadecylamine grafting. CFs that were functionalized with PDA and then reacted with octadecylamine were thoroughly characterized. To illustrate applications of this functionalization strategy, we incorporated the functionalized CFs into polar and nonpolar polymers as reinforcing fillers, with epoxy resin and poly(ethylene-co-octene) as example matrices. The detailed functionalization and fabrication processes are illustrated in Scheme 1. The satisfactory effect was identified by the excellent interfacial interaction between functionalized fibers and polymer matrices, which indicated that our strategy has a promising future in the industrial field.

## 2. EXPERIMENTAL DETAILS

**2.1. Materials.** Short carbon fibers (SCFs) (T700 12K) with a mean diameter of 10 $\mu$m and a length of 200 $\mu$m were produced by Toray Industries Inc. (Japan). According to the supplier, the as-received SCFs are coated with commercial polyurethane sizing. Hydroxyphenethylamine hydrochloride (dopamine, 98%) and tris-(hydroxy-methyl) aminomethane (TRIS, 99%), which is used as a buffer agent, were purchased from Sigma-Aldrich. Octadecylamine (ODA) and triethylamine were purchased from Aladdin Reagent Corp. (Shanghai, China). EXACT 5062 poly(ethylene-co-octene) (POE) is a commercial grade product produced by ExxonMobil Chemical Co. with density of 860 kg/m$^3$ and melt index of 0.50 g/10 min (190 °C, 2.16 kg). E51 epoxy resin (EP), whose viscosity and epoxide value are ~2500 mPa s (40 °C) and 0.48−0.54 eq/100 g, was purchased from Bluestar Wuxi Petrochemical Co. Ltd. (Jiangsu, China). Triethylenetetramine (TETA), the curing agent of EP, was purchased from Aladdin Reagent Corp. (Shanghai, China). All chemical reagents and solvents were used as received and without further purification.

**2.2. Surface Functionalization of SCFs.** The as-received SCFs were first heated in a tubular furnace at 550 °C for 1 h under an argon atmosphere to remove the commercial sizing before being used, which were denoted as desized-SCFs.

To prepare hydrophilic SCFs, typically, 30 g of desized-SCFs were immersed in 1500 mL of buffer solution, followed by the addition of three g of dopamine. After sonication for 10 min, the mixture was then put under magnetic stirring at room temperature for 24 h. pH-induced self-polymerization of dopamine produced PDA coating on the surface of desized-SCFs. The buffer solution was prepared with 10 mM TRIS and its pH was adjusted to 8.5 with 1 M hydrochloric acid, monitored by a pH meter. The PDA-coated SCFs (PDA-SCFs) were collected via filtration and washed with deionized water 3 times to remove free dopamine and PDA before being dried in a vacuum oven at 50 °C for 24 h.

To obtain oleophilic SCFs, PDA-SCFs reacted with ODA through amine-catechol adduct formation. Exemplarily, 20 g of PDA-SCFs was immersed in 2000 mL of ethanol containing 20 mM triethylamine; 5.4 g of ODA was subsequently added and stirred for 24 h. After being collected and rinsed three times with ethanol to remove unreacted ODA, the ODA-functionalized SCFs (C18-PDA-SCFs) were dried at 50 °C under a vacuum for 24 h.

**2.3. Characterization of SCFs.** Scanning electron microscopy (SEM, TESCAN 5136 MM) was applied to observe the surface morphologies of the SCFs at an operating voltage of 20 kV. A Dataphysics OCA 40 instrument was used to measure the surface wettability of the SCFs. Before being measured, the SCFs were pressed to plane shape on a polytetrafluoroethylene coated glass slide using a hydraulic jack. Fourier transform infrared (FTIR) spectra were recorded using a Nicolet spectrometer. Thermogravimetric analysis (TGA) was carried out under nitrogen atmosphere with a Perkin-Elmer Thermal Analyzer from 50 to 800 °C at a heating rate of 20 °C min$^{-1}$. X-ray photoelectron spectroscopy (XPS, Kratos AXIS

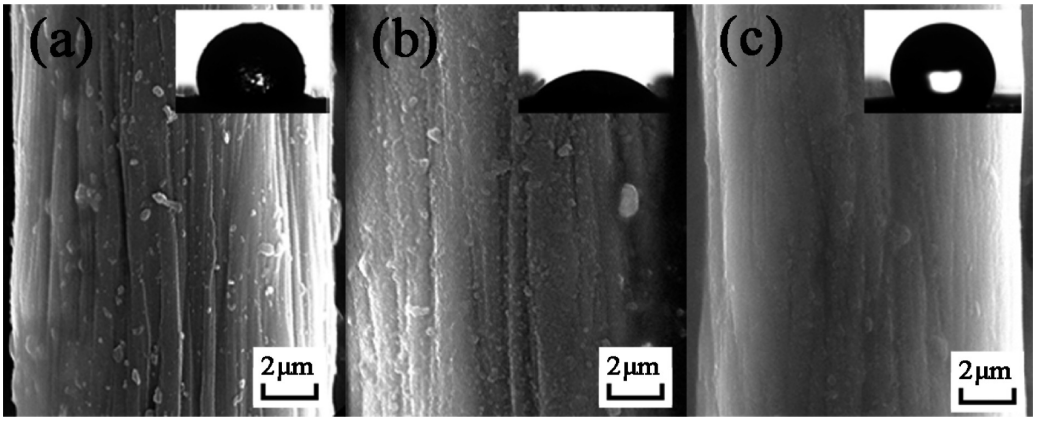


**Figure 1.** SEM images of the surfaces of (a) desized-SCFs, (b) PDA-SCFs, and (c) C18-PDA-SCFs. The insets are the water contact angle (WCA) of SCFs.

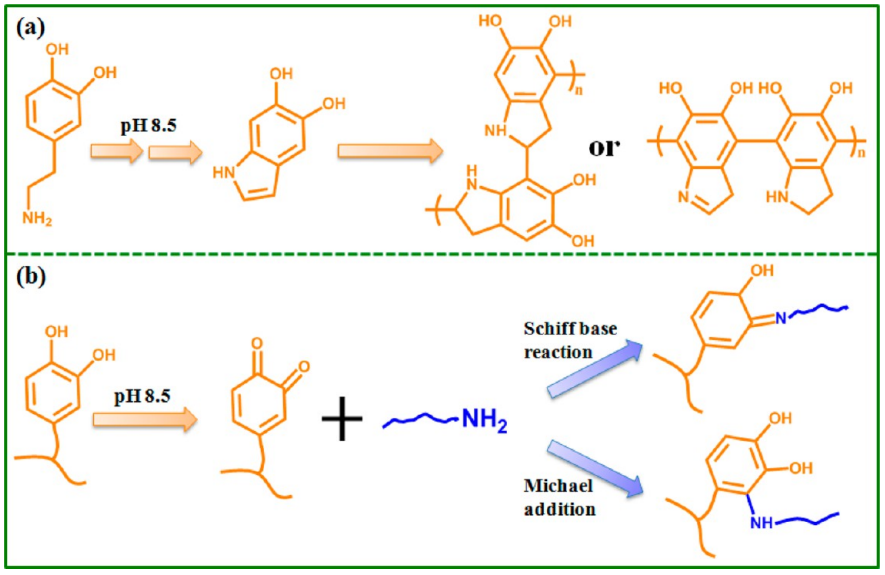


**Figure 2.** Reaction mechanism of (a) dopamine and (b) ODA in dip-coating process.

Ultra$^{DLD}$) was used to determine the chemical composition of the SCFs (for more details, see the Supporting Information).

**2.4. Preparation and Properties Measurement of SCF/Polymer Composites.** To prepare PDA-SCF/EP composites, we mixed 15 wt % PDA-SCFs (11% in volume fraction) with epoxy at 60 °C for 30 min. After curing agent (TETA) was added, the mixture was then stirred for 10 min and poured into the preheated dog-bone type Teflon molds, followed by curing at 100 °C for 2 h. For comparison, desized-SCFs/EP composites and neat EP were also prepared using the same procedure. To obtain C18-PDA-SCF/POE composite, 15 wt % C18-PDA-SCFs (7.8% in volume fraction) was melt mixed with POE using a Haake-Rheomix at 150 °C for 8 min with a screw speed of 90 rpm. Subsequently, this sample was compression molded (150 °C, 5 MPa) into 2 mm thick sheets and cut into dog-bone type specimens for the tensile test. Following the similar procedure, neat POE and desized-SCF/POE specimens were prepared as references.

Mechanical properties were measured at 23 °C and ~40% relative humidity using a SANS CMT-4102 universal testing machine (Shenzhen, China) with an extensometer (25 mm) at a crosshead speed of 2 and 500 mm/min for EP and POE specimens, respectively. All the specimens have a dimension of 75 mm (length) × 12.5 mm (width) × 25 mm (narrow portion length) × 4.0 mm (narrow portion width) × 2.0 mm (thickness). At least five tests were performed for each sample, from which mean values and standard deviations were derived. The tensile-fractured surfaces were observed by TESCAN 5136 MM SEM. Dynamic mechanical analysis (DMA, Mettler-Toledo DMA/SDTA861e) were conducted to measure the storage modulus and glass transition temperature ($T_g$) of composites. The dimensions of both EP and POE specimens for DMA measurements were 25 mm (length) × 4.0 mm (width) × 2.0 mm (thickness). The testing was performed in single cantilever mode between 50 and 200 °C for EP and in tension mode from −80 to 20 °C for POE specimens. All measurements were conducted at a frequency of 1 Hz and a heating rate of 5 °C/min.

## 3. RESULTS AND DISCUSSION

**3.1. Surface Functionalization and Characterization of SCFs.** The surface topographies of the SCFs were observed using SEM. Figure 1a displays ridges and striations along the fiber axis on the surface of desized-SCFs. By contrast, the surface wrinkles of PDA-SCFs become invisible (Figure 1b), indicating the presence of PDA film. As shown in Figure 1c, the smooth surface of C18-PDA-SCFs is dramatically different from the two above-mentioned SCFs, the wrinkles of which can be hardly seen. It suggests that the surface of PDA-SCFs was further covered with ODA coating. The insets show the water contact angle (WCA) of SCFs. The WCA of desized-SCFs is 110°, whereas that of PDA-SCFs is 45°, implying that PDA treatment significantly improves hydrophilicity in accordance with the appearance of PDA coating on the PDA-SCF surface.


dx.doi.org/10.1021/am404394g | ACS Appl. Mater. Interfaces 2014, 6, 349−356

After reacting with ODA, WCA change from 45 to 123°, which confirms that ODA layer was grafted onto the surface of PDA-SCFs. It is also in agreement with the discussion of SEM images. All of these results suggest that carbon fibers are successfully transformed from amphiphobic to hydrophilic by coating with PDA film and further inverted to oleophilic after following ODA grafting.

In our strategy, both of hydrophilic and oleophilic functionalization are achieved through the simple dip-coating approach. For hydrophilic functionalization, desized-SCFs were soaked in the buffer solution of dopamine with pH 8.5. According to previous research,[34−40] the catechol groups of dopamine are easily oxidized at weak alkaline pH, resulting in a quinone structure, which then forms 5, 6-dihydroxyindole by nucleophilic reaction and rearrangement. Further oxidation causes intermolecular cross-linking to yield thin PDA layer on the substrate surface (Figure 2a). In this work, PDA film was deposited on the surface of desized-SCFs through a similar reaction, introducing polar groups such as hydroxyl and imine. Compared with the amphiphobic surface of desized-SCFs, polar groups give PDA-SCFs their hydrophilic properties, consistent with the results of WCA. In terms of oleophilic treatment, PDA-SCFs were immersed in ODA solution containing triethylamine, and after 24 h stirring, ODA was grafted onto the surface of PDA-SCFs. During stirring, the oxidized quinone form of catechol groups can react with amines via Michael addition or Schiff base reaction, which has been proved by Kang et al.[21] and Ball et al.[30] Accordingly, hydrophobic alkyl chains can be grafted onto the PDA film, which inverts hydrophilic to oleophilic (Figure 2b).

Direct evidence for our successful surface functionalization of SCFs was provided by FTIR spectra, as shown in Figure 3. For

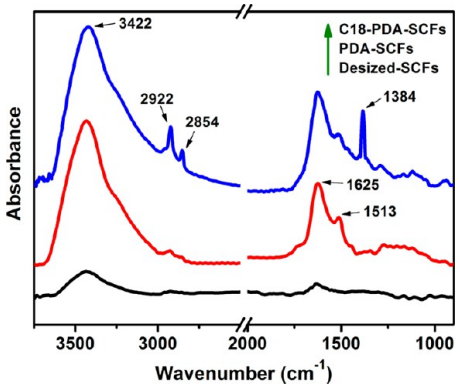


**Figure 3.** FTIR spectra of desized-SCFs, PDA-SCFs, and C18-PDA-SCFs.

desized-SCFs, there are two weak absorption bands at 1625 and 3422 $cm^{-1}$, which should be attributed to aromatic C═C and O−H stretching vibration. Upon coating with PDA, the band around 3422 $cm^{-1}$ becomes stronger and broader. A similar result has been obtained by Zhu, who ascribed this broadened peak to both catechol O−H stretching vibration and N−H stretching vibration from PDA layer.[41] Moreover, the new absorption peak of PDA-SCFs at 1513 $cm^{-1}$, assigned to N−H shearing vibration of PDA, provides further evidence for the successful coating, consistent with the FTIR analyses of PDA homopolymer and dopamine monomer (see Figure S1 in the Supporting Information). In the spectrum of C18-PDA-SCFs, the doublet at 2922 and 2854 $cm^{-1}$ associated with C−H stretching vibration is extremely high. It suggests the presence of ODA on the surface because the grafted ODA chains are rich in methyl and methylene groups. Furthermore, C18-PDA-SCFs also exhibit a new distinct band at 1384 $cm^{-1}$, which corresponds to the shearing vibration of C═N groups connected with aromatic rings. This absorption cannot be observed in the spectrum of pure ODA (see Figure S1 in the Supporting Information), implying that part of the PDA film reacted with ODA via Michael addition. The FTIR results confirm the PDA coating on PDA-SCF surface and the covalent bonding between PDA coating and ODA in C18-PDA-SCFs.

Thermogravimetric curves of SCFs, PDA, and ODA are presented in Figure 4. As to desized-SCFs, weight loss was not observed throughout the temperature range investigated (50−800 °C), indicating the high thermal stability of neat carbon fibers. By contrast, PDA-SCFs and C18-PDA-SCFs show evident decomposition under the same calcination procedure. PDA-SCFs start to lose weight at around 300 °C, which is in good agreement with the decomposition of PDA homopolymer (Figure 4b). As suggested by Zhu, this mass loss peak should be attributed to the decomposition of PDA main chain.[41] It is worth nothing that the mass of PDA residue is as high as ∼50 wt %, which derives from its high residual rate during pyrolysis. For PDA-SCFs, the weight loss is about 2 wt %, suggesting that ∼4 wt % PDA is coated on the surface. In the TG traces of C18-PDA-SCFs, weight loss at temperatures observed up to about 200 °C is associated with the decomposition of ODA chain, which is in consistent with that of neat ODA. Compared with desized-SCFs, the weight losses of the PDA-SCFs and C18-PDA-SCFs at lower temperature also support the conclusion that PDA and ODA were successfully coated onto the surface of SCFs.

The surface chemical compositions of SCFs were further analyzed using XPS. For desized-SCFs, the XPS C 1s core-level spectrum can be curve-fitted with four peak components at the binding energies (BEs) of about 284.7, 285.5, 286.0, 287.6, and 289.1 eV, attributable to the C−C, C−N, C−O, C═O, and O−C═O species, respectively (Figure 5a). The weak peak component of C−N species is attributed to pyrrole and pyridine structures, which are formed during preoxidation and carbonization of polyacrylonitrile fibers, on carbon fibers. Figure 5b shows that the N 1s core level spectrum of desized-SCFs can be curved into only two peak components with BEs at about 398.8 and 401.7 eV, attributable to the −N═ and $N^+$ species.[42,43] It further verifies the discussion of the C 1s core-level spectrum. After PDA coating, the intensities of N 1s and O 1s peak signals become much stronger in the wide scan spectra (see Figure S2a, b in the Supporting Information). In the N 1s core-level spectrum of PDA-SCFs, the intensities of −N═ and $N^+$ peak component dramatically decrease and a new intense peak component appears at the BEs of 399.8 eV, assigned to −NH− species. The C 1s core-level spectral line shape of PDA-SCFs is similar to that of pure PDA[21] and is consistent with the structure of PDA,[44] whose theoretical C−C:C−N:C−O ratio is 4:2:2. In particular, the [N]/[C] ratio of the PDA-SCF surface is 0.095 (Table 1), close to the value of 0.11 in Kang's report[45] and the theoretic value of 0.125 for dopamine. These results confirm the success in obtaining PDA-SCFs. As to C18-PDA-SCFs, Figure S2c in the Supporting Information shows that the intensities of N1s and O1s peak signals are weaker than that of PDA-SCFs in the wide scan spectra. The [N]/[C] ratio of the C18-PDA-SCF surface is 0.073 (Table 1), between the theoretic value of 0.055 for ODA

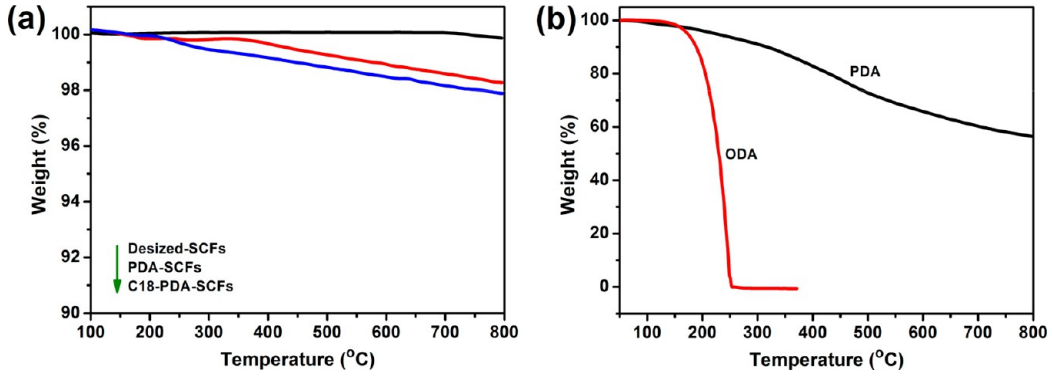


**Figure 4.** TGA traces of (a) desized-SCFs, PDA-SCFs, and C18-PDA-SCFs; (b) PDA and ODA.

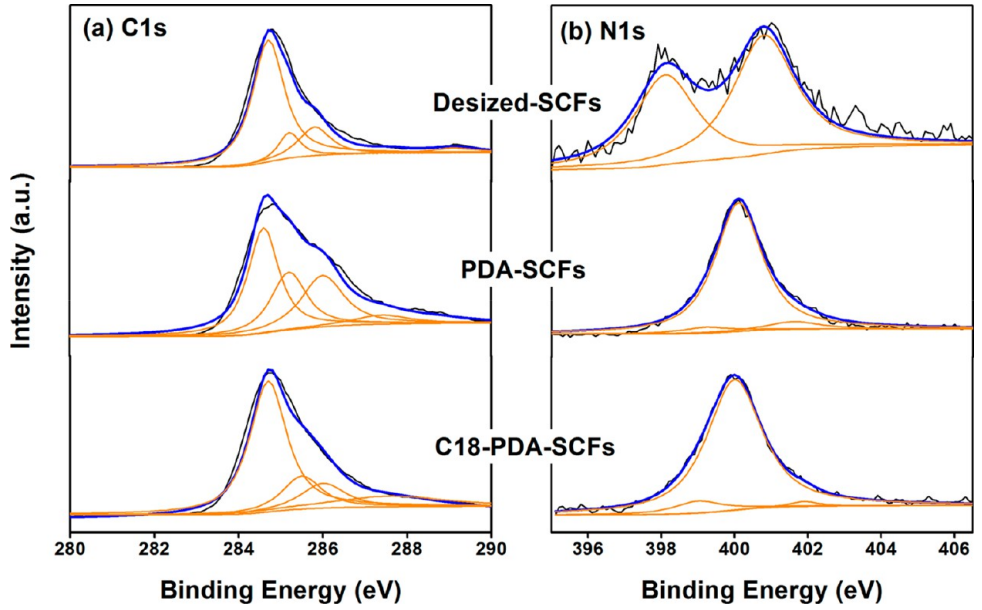


**Figure 5.** (a) C1s and (b) N1s spectra of desized-SCFs, PDA-SCFs, and C18-PDA-SCFs.

**Table 1. Relative Concentration of Compositional Atoms and Nitrogen-Containing Functional Groups for Desized-SCF, PDA-SCF, and C18-PDA-SCF Samples**

| | atomic composition (%) | | | | | | |
|---|---|---|---|---|---|---|---|
| samples | carbon | oxygen | nitrogen | −N= (%) | −NH− (%) | $N^+$ (%) | N/C atomic ratio |
| desized-SCFs | 70.32 | 10.79 | 2.95 | 43.0 | | 57.0 | 0.042 |
| PDA-SCFs | 71.25 | 19.12 | 6.72 | 4.3 | 89.7 | 6.0 | 0.095 |
| C18-PDA-SCFs | 78.54 | 13.52 | 5.78 | 7.3 | 90.9 | 1.8 | 0.073 |

and 0.125 for dopamine, implying the ODA layer is partly covered on the surface. To investigate ODA grafting, we focus on the N 1s spectrum of the C18-PDA-SCFs. The increase in intensity of −N= peak component suggests the formation of Schiff base, which proves that the reaction between PDA coating and ODA is successful. Taken together, all these results verify that PDA and ODA layers were deposited on PDA-SCF and C18-PDA-SCF surfaces.

**3.2. Application of Functionalized SCFs in Polymer Composites.** To illustrate applications of our functionalization strategy, we respectively introduced PDA-SCFs and C18-PDA-SCFs into polar and nonpolar polymer, with EP and POE as examples. The reinforcing effect of functionalized SCFs on composites is first evaluated by tensile testing (for stress−strain curves, see Figure S3 in the Supporting Information). The tensile strength and Young's modulus strength data are presented in Figure 6. For EP composites (Figure 6a, b), the incorporation of desized-SCFs brings about only 35 and 75% increases in tensile strength and Young's modulus (76.0 ± 4.0 MPa and 4.1 ± 0.3 GPa). By comparison, the increases are up to 70 and 130%, respectively, for PDA-SCFs/EP (95.0 ± 5.2 MPa and 5.5 ± 0.4 GPa). As to POE composites (Figure 6d, e), the introduction of desized-SCFs into POE host lead to a 35% raise in tensile strength (4.5 ± 0.4 MPa) and a 68% increase in Young's modulus (3.6 ± 0.4 MPa). Comparably, more prominent improvement, namely 60% increase in tensile strength (5.3 ± 0.2 MPa) and 160% rise in Young's modulus (5.6 ± 0.2 MPa), results from the incorporation of C18-PDA-SCFs. In a previous study, Fan et al. prepared carbon fiber reinforced epoxy composites with a functionalized sizing.[12]


dx.doi.org/10.1021/am404394g | ACS Appl. Mater. Interfaces 2014, 6, 349−356

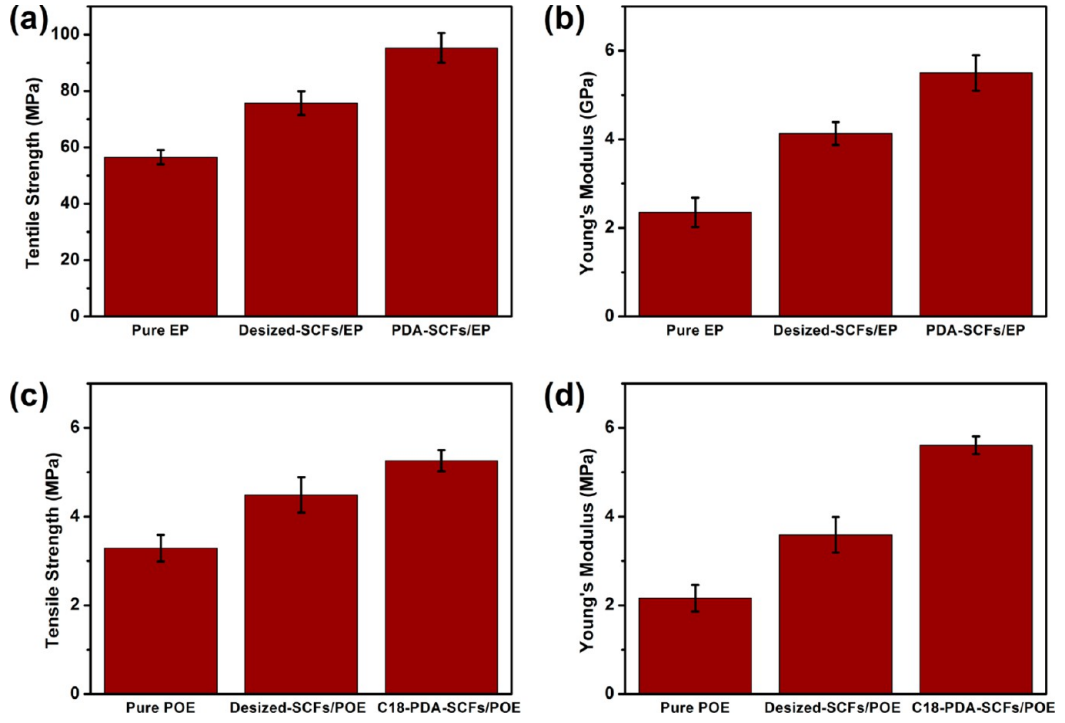


**Figure 6.** (a) Tensile strength and (b) Young's modulus of pure EP, desized-SCF/EP, and PDA-SCF/EP composites. (c) Tensile strength and (d) Young's modulus of pure POE, desized-SCF/POE, and C18-PDA-SCF/POE composites.

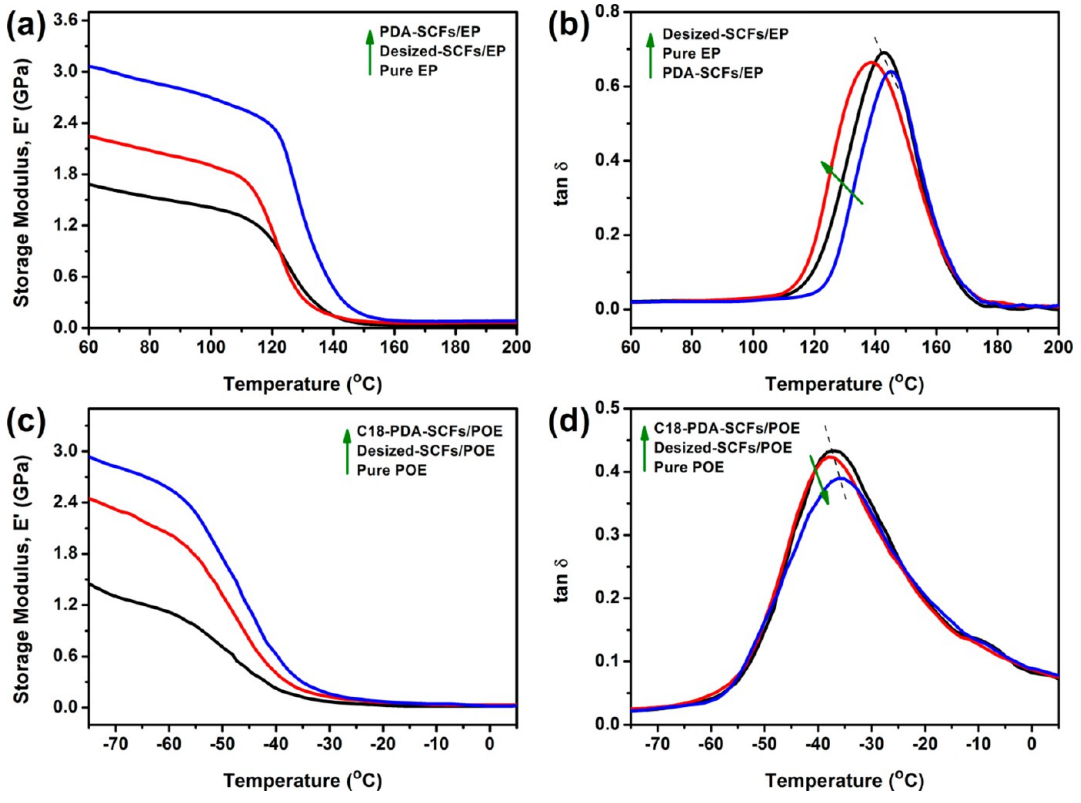


**Figure 7.** (a) Storage modulus ($E'$) and (b) tan $\delta$ vs temperature curves of pure EP, desized-SCF/EP, and PDA-SCF/EP composites. (c) Storage modulus ($E'$) and (d) tan $\delta$ vs temperature curves of pure POE, desized-SCF/POE, and C18-PDA-SCF/POE composites.

They evidenced that strong interfacial bonding, which allows efficient stress transfer from matrix to fibers, led to higher tensile properties for optimized modified carbon fiber reinforced composites (34 and 23% higher than pristine carbon fiber reinforced composites in tensile strength and elastic modulus). In the present work, compared with desized-SCFs/EP, the increase of tensile strength and elastic modulus were 25 and 33% for PDA-SCFs/EP, which is comparable to the


dx.doi.org/10.1021/am404394g | ACS Appl. Mater. Interfaces 2014, 6, 349−356

improvement in Fan et al.'s study. The evident improvements of the mechanical properties for functionalized SCFs filled composites demonstrate that PDA-based functionalization can produce satisfactory effect in interfacial adhesion. These results also confirm the success of coating PDA and ODA onto the SCF surfaces.

DMA is also a powerful tool to investigate the mechanical properties of polymers. The DMA results of EP and POE composites are given in Figure 7, which exhibit evident changes in dynamic mechanical behavior for desized and functionalized SCFs reinforced composites, compared with the neat polymer sample at a temperature range below $T_g$. As shown in Figure 7a, the storage modulus of desized-SCFs/EP is higher than that of neat EP. Among these three samples, the PDA-SCFs/EP has the highest storage modulus, consistent with the results of tensile testing. As to Figure 7b, it is interesting to note that the $T_g$ of composites decrease after the addition of desized-SCFs. In previous works,[46−48] a similar result have also been reported and it was attributed to the influence of the normal curing reaction between the hardener and matrix resin by fillers, resultantly decreasing the cross-link density. However, PDA-SCF/EP composites have a relatively higher $T_g$ than neat EP, indicating that restricting effect of matrix chain molecular mobility,[49] which may be caused by favorable interfacial adhesion between fillers and host, plays a primary part in PDA-SCFs/EP. For POE samples (Figure 7c, d), the increasing trends of storage modulus and $T_g$ are similar to that of EP specimens.

To directly investigate the interfacial adhesion in SCFs/EP and SCFs/POE, we took SEM observations on the tensile-fractured surfaces of composites, as shown in Figure 8. It is obvious that pull-out and debonding between desized-SCFs and EP matrix as well as the smooth desized-SCF surface without remnants of resin can be found in Figure 8a, b. However, Figure 8c, d show almost seamless interfaces between PDA-SCFs and EP matrix, and few PDA-SCFs were pulled out from the host. These results show that PDA-SCFs possess excellent interfacial adhesion with EP host. According to Yang, the interfacial interactions between PDA coating and EP matrix are dominated by the hydrogen bonds between catechol groups and epoxy groups. Other possible interactions include the covalent bonding between amine groups of the hardener and PDA layer as well as the bond between epoxy molecules and imine groups of PDA.[17] As to desized-SCFs/POE, images e and f in Figure 8 show a mostly clean fiber−matrix interface failure path, whereas for the C18-PDA-SCFs/POE in images g and h in Figure 8, the POE remains attached to fibers. It confirms that interfacial adhesion of C18-PDA-SCFs/POE improves as a result of the good compatibility between oleophilic ODA chains and POE host. Therefore, SEM observations testify that PDA-based functionalization can efficiently improve the interfacial adhesion between carbon fibers and polymers matrices.

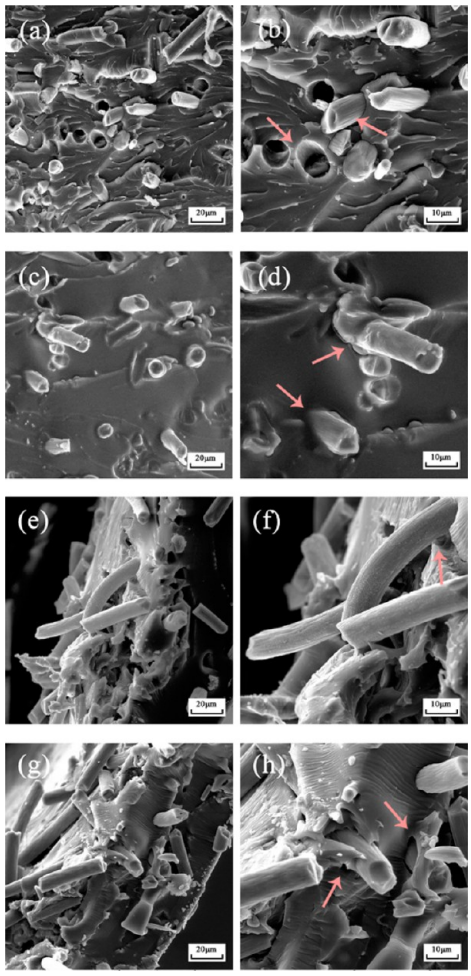


**Figure 8.** SEM micrographs of the tensile-fractured surfaces for (a, b) desized-SCF/EP composites, (c, d) PDA-SCF/EP composites, (e, f) desized-SCF/POE composites, and (g, h) PDA-SCF/POE composites.

## 4. CONCLUSION

In summary, we develop an efficient and robust route to functionalize carbon fibers based on dopamine chemistry, such as hydrophilic and oleophilic functionalization. With PDA coating and further ODA grafting, the WCA of SCFs changed from 110 to 45° and then to 123°, showing that carbon fibers were successfully converted from amphiphobic to hydrophilic and then oleophilic. To illustrate applications of this functionalization, PDA-SCFs and C18-PDA-SCFs were respectively introduced into polar polymer and nonpolar polymer, with EP and POE as example. The remarkably improved mechanical properties of the resulting composites indicated that PDA-based functionalization could achieve satisfactory reinforcing effect. Therefore, our work provides a general pathway to specifically functionalize carbon fibers that is of great interest to the industrial field.

## ■ ASSOCIATED CONTENT

### Ⓢ Supporting Information

FTIR spectra of ODA, PDA, and dopamine; XPS wide scan spectra of desized-SCFs, PDA-SCFs, and C18-PDA-SCFs; typical stress−strain curves of EP and POE composites. This material is available free of charge via the Internet at http://pubs.acs.org/.

## ■ AUTHOR INFORMATION

### Corresponding Author

*E-mail: jcfeng@fudan.edu.cn. Tel: 86 (21) 6564 3735. Fax: +86- 21-6564 0293.

### Notes

The authors declare no competing financial interest.

## ■ ACKNOWLEDGMENTS

This work was financially supported by the Natural Science Foundation of China (21174032 and 51373042) and National Basic Research Program of China (2011CB605704).

## ■ REFERENCES

(1) Chung, D. D. L., In *Composite Materials*, 2nd ed.; Derby, B., Ed. Springer: London, 2010; p 170.
(2) Atkinson, K. E.; Kiely, C. *Compos. Sci. Technol.* **1998**, *58*, 1917−1922.
(3) Ageorges, C.; Friedrich, K.; Ye, L. *Compos. Sci. Technol.* **1999**, *59*, 2101−2113.
(4) Zhao, J.; Liu, L.; Guo, Q.; Shi, J.; Zhai, G.; Song, J.; Liu, Z. *Carbon* **2008**, *46*, 380−383.
(5) Chen, X.; Farber, M.; Gao, Y.; Kulaots, I.; Suuberg, E. M.; Hurt, R. H. *Carbon* **2003**, *41*, 1489−1500.
(6) Severini, F.; Formaro, L.; Pegoraro, M.; Posca, L. *Carbon* **2002**, *40*, 735−741.
(7) Fukunaga, A.; Ueda, S. *Compos. Sci. Technol.* **2000**, *60*, 249−254.
(8) Pittman, C. U.; Jiang, W.; Yue, Z. R.; Gardner, S.; Wang, L.; Toghiani, H.; Leon, Y.; Leon, C. A. *Carbon* **1999**, *37*, 1797−1807.
(9) Wu, G. M. *Mater. Chem. Phys.* **2004**, *85*, 81−87.
(10) Montes-Morán, M. A.; Van Hattum, F. W. J.; Nunes, J. P.; Martínez-Alonso, A.; Tascón, J. M. D.; Bernardo, C. A. *Carbon* **2005**, *43*, 1795−1799.
(11) Downs, W. B.; Baker, R. T. K. *J. Mater. Res.* **1995**, *10*, 625−633.
(12) Zhang, X.; Fan, X.; Yan, C.; Li, H.; Zhu, Y.; Li, X.; Yu, L. *ACS Appl. Mater. Interfaces* **2012**, *4*, 1543−1552.
(13) Tang, L. G.; Karoos, J. L. *Polym. Compos.* **1997**, *18*, 100−113.
(14) Xie, J.; Xin, D.; Cao, H.; Wang, C.; Zhao, Y.; Yao, L.; Ji, F.; Qiu, Y. *Surf. Coat. Technol.* **2011**, *206*, 191−201.
(15) Waite, J. H.; Qin, X. *Biochemistry* **2001**, *40*, 2887−2893.
(16) Lee, H.; Dellatore, S. M.; Miller, W. M.; Messersmith, P. B. *Science* **2007**, *318*, 426−430.
(17) Yang, L.; Phua, S. L.; Teo, J. K.; Toh, C. L.; Lau, S. K.; Ma, J.; Lu, X. *ACS Appl. Mater. Interfaces* **2011**, *3*, 3026−3032.
(18) Phua, S. L.; Yang, L.; Toh, C. L.; Huang, S.; Tsakadze, Z.; Lau, S. K.; Mai, Y. W.; Lu, X. *ACS Appl. Mater. Interfaces* **2012**, *4*, 4571−4578.
(19) Huang, S.; Yang, L.; Liu, M.; Phua, S. L.; Yee, W. A.; Liu, W.; Zhou, R.; Lu, X. *Langmuir* **2013**, *29*, 1238−1244.
(20) Phua, S. L.; Yang, L.; Toh, C. L.; Ding, G.; Lau, S. K.; Dasari, A.; Lu, X. *ACS Appl. Mater. Interfaces* **2013**, *5*, 1302−1309.
(21) Xu, L.; Yang, W.; Neoh, K. G.; Kang, E. T.; Fu, G. *Macromolecules* **2010**, *43*, 8336−8339.
(22) Kaminska, I.; Das, M. R.; Coffinier, Y.; Niedziolka-Jonsson, J.; Sobczak, J.; Woisel, P.; Lyskawa, J.; Opallo, M.; Boukherroub, R.; Szunerits, S. *ACS Appl. Mater. Interfaces* **2012**, *4*, 1016−1020.
(23) Tian, Y.; Cao, Y.; Wang, Y.; Yang, W.; Feng, J. *Adv. Mater.* **2013**, *25*, 2980−2983.
(24) Rim, N. G.; Kim, S. J.; Shin, Y. M.; Jun, I.; Lim, D. W.; Park, J. H.; Shin, H. *Colloid. Surf. B* **2012**, *91*, 189−197.
(25) Son, H. Y.; Ryu, J. H.; Lee, H.; Nam, Y. S. *ACS Appl. Mater. Interfaces* **2013**, *5*, 6381−6390.
(26) Son, H. Y.; Ryu, J. H.; Lee, H.; Nam, Y. S. *Macromol. Mater. Eng.* **2013**, *298*, 547−554.
(27) Bernsmann, F.; Richert, L.; Senger, B.; Lavalle, P.; Voegel, J. C.; Schaaf, P.; Ball, V. *Soft Matter* **2008**, *4*, 1621−1624.
(28) Lee, H.; Rho, J.; Messersmith, P. B. *Adv. Mater.* **2009**, *21*, 431−434.
(29) Ou, J.; Wang, J.; Liu, S.; Zhou, J.; Yang, S. *J. Phys. Chem. C* **2009**, *113*, 20429−20434.
(30) Bernsmann, F.; Frisch, B.; Ringwald, C.; Ball, V. *J. Colloid Interface Sci.* **2010**, *344*, 54−60.
(31) Kang, S. M.; You, I.; Cho, W. K.; Shon, H. K.; Lee, T. G.; Choi, I. S.; Karp, J. M.; Lee, H. *Angew. Chem., Int. Ed.* **2010**, *49*, 9401−9404.
(32) Niu, H.; Wang, S.; Zeng, T.; Wang, Y.; Zhang, X.; Meng, Z.; Cai, Y. *J. Mater. Chem.* **2012**, *22*, 15644−15653.
(33) Cao, Y.; Zhang, X.; Tao, L.; Li, K.; Xue, Z.; Feng, L.; Wei, Y. *ACS Appl. Mater. Interfaces* **2013**, *5*, 4438−4442.
(34) Waite, J. H. *Nat. Mater.* **2008**, *7*, 8−9.
(35) Park, T. J.; Kim, J.; Kim, T. K.; Park, H. M.; Choi, S. S.; Kim, Y. *Bull. Kor. Chem. Soc.* **2008**, *29*, 2459−2464.
(36) Adhyaru, B. B.; Akhmedov, N. G.; Katritzky, A. R.; Bowers, C. R. *Magn. Reson. Chem.* **2003**, *41*, 466−474.
(37) Arzillo, M.; Pezzella, A.; Crescenzi, O.; Napolitano, A.; Land, E. J.; Barone, V.; D'Ischia, M. *Org. Lett.* **2010**, *12*, 3250−3253.
(38) Bisaglia, M.; Mammi, S.; Bubacco, L. *J. Biol. Chem.* **2007**, *282*, 15597−15605.
(39) D'Ischia, M.; Napolitano, A.; Pezzella, A.; Meredith, P.; Sarna, T. *Angew. Chem., Int. Ed.* **2009**, *48*, 3914−3921.
(40) Ball, V.; Del Frari, D.; Michel, M.; Buehler, M. J.; Toniazzo, V.; Singh, M. K.; Gracio, J.; Ruch, D. *BioNanoSci.* **2012**, *2*, 16−34.
(41) Zhu, L.; Lu, Y.; Wang, Y.; Zhang, L.; Wang, W. *Appl. Surf. Sci.* **2012**, *258*, 5387−5393.
(42) Gammon, W. J.; Kraft, O.; Reilly, A. C.; Holloway, B. C. *Carbon* **2003**, *41*, 1917−1923.
(43) Lin, M.; Huang, H.; Liu, Y.; Liang, C.; Fei, S.; Chen, X.; Ni, C. *Nanotechnology* **2013**, *24*, No. 065501.
(44) Cui, J.; Wang, Y.; Postma, A.; Hao, J.; Hosta-Rigau, L.; Caruso, F. *Adv. Funct. Mater.* **2010**, *20*, 1625−1631.
(45) Yang, W.; Cai, T.; Neoh, K. G.; Kang, E. T.; Dickinson, G. H.; Teo, S. L. M.; Rittschof, D. *Langmuir* **2011**, *27*, 7065−7076.
(46) Dong, S.; Gauvin, R. *Polym. Compos.* **1993**, *14*, 414−420.
(47) Lee, J. M.; Kim, S. J.; Kim, J. W.; Kang, P. H.; Nho, Y. C.; Lee, Y. S. *J. Ind. Eng. Chem.* **2009**, *15*, 66−71.
(48) Luo, Y.; Zhao, Y.; Cai, J.; Duan, Y.; Du, S. *Mater. Des.* **2012**, *33*, 405−412.
(49) Brocks, T.; Cioffi, M. O. H.; Voorwald, H. J. C. *Appl. Surf. Sci.* **2013**, *274*, 210−216.